GEOPHYSICAL RESEARCH LETTERS, VOL. 23, NO. 15, PAGES 1897-1900, JULY 15, 1996

# GPS detection of ionospheric perturbations following a Space Shuttle ascent

Eric Calais[1] and J. Bernard Minster
Scripps Institution of Oceanography, La Jolla, CA

**Abstract.** The exhaust plume of the Space Shuttle during its ascent is a very powerful source of energy that excites atmospheric acoustic perturbations. Because of the coupling between neutral particles and electrons at ionospheric altitudes, these low frequency acoustic perturbations induce variations of the ionospheric electron density. We computed ionospheric electron content time series using Global Positioning System data collected on Bermuda island during the STS-58 Space Shuttle launch. The analysis of these time series shows a perturbation of the ionospheric electron content following the launch and lasting for 35 mn, with periods less than 10 mn. The perturbation is complex and shows two sub-events separated by about 15 mn at 200 km from the source. The phase velocities and waveform characteristics of the two sub-events lead us to interpret the first impulsive arrival as the direct propagation of the shock wave front, followed by oscillatory guided waves probably excited by the primary shock wave and propagating along horizontal atmospheric interfaces at 120 km altitude and below.

## Introduction

After the initial ascent phase of its flight, the Space Shuttle accelerates almost horizontally at an altitude of about 110 km in order to reach its assigned orbit. This horizontal acceleration lasts for about 5 minutes; the shuttle is powered by its main engine and its speed increases from 2.5 km/s to 7.5 km/s. The exhaust plume of the main engine burn represents a source of $2\times10^{12}$ Joules of energy that explodes in the upper atmosphere along the shuttle trajectory and generates long-period (>30 sec) acoustic perturbations (Noble, 1990; Li *et al.*, 1994). Because of the coupling between neutral and ionized atmosphere at ionospheric heights (McLeod, 1966), these perturbations induce fluctuations of the ionospheric electron density. The Global Positioning System (GPS) provides a way of directly measuring the Total Electron Content (TEC) in the ionosphere (Klobuchar, 1985) and, therefore, of detecting acoustic and gravity perturbations in the upper atmosphere (Calais and Minster, 1995). In this work, we use GPS measurements taken in Bermuda on October 18, 1993, to detect and analyze the atmospheric perturbation caused by the STS-58 Space Shuttle ascent.

[1]Now at CNRS, Sophia Antipolis, France



Paper number 96GL01256
0094-8534/96/96GL-01256$05.00

## Data and Method

On October 18, 1993, the Space Shuttle Columbia was launched from Kennedy Space Center (Cape Canaveral, Florida) for the STS-58 mission (Fig. 1). The shuttle lifted off at 14:53:10 UT ($t_o$), the solid rocket boosters were separated from the external tank at $t_o$ + 123.8 *sec*, the main engine cut off occured at $t_{MECO} = t_o + 515.56$ *sec*. The quasi-horizontal acceleration part of the ascent lasted from $t_1 = t_o + 210$ *sec* to $t_{MECO}$, *i.e.* about 5 minutes. During this ascent, the shuttle headed east-north-east and flew as close as 200 km to a GPS station operating permanently on Bermuda island (Fig. 1). This station is equiped with a TurboRogue GPS receiver sampling at 30 sec intervals. The satellite displacements during the 306 sec time span between $t_1$ and $t_{MECO}$ are very small and will not be a factor in the following analysis.

The radio signals broadcast at 1.57542 GHz ($f_1$, wavelength $\lambda_1$) and 1.2276 GHz ($f_2$, $\lambda_2$) by the GPS satellites are dispersively delayed along their path by interactions with free electrons in the ionosphere. Since the differential delay between the $f_1$ and $f_2$ frequencies is proportional to the electron density along the ray path (Klobuchar, 1985), phase and P-code delays recorded on the two GPS frequencies allow for direct measurements of the ionospheric electron density, integrated along the line-of-sight between the receiver and the satellite. The processing technique used in this work to compute ionospheric Total Electron Content (TEC) from GPS phase and code data has been published elsewhere (Calais and Minster, 1995). We refer the reader to this publication for further explanations.

## The TEC perturbation

We processed the GPS data from all available GPS satellites recorded at Bermuda in a time window extending from 2 hours before the shuttle launch to 4 hours after. The calculations were carried out at each sampling point (every 30 sec) and provide raw TEC time series (Fig 2). The TEC time series are dominated by high amplitude variations with periods of several hours related to the daily solar cycle and to the motion of the satellites in latitude and longitude. We eliminated these long periods by applying a 0.003 Hz cutoff high-pass filter to the raw time series. The filtered time series (Fig 2) show a strong amplitude perturbation for satellites GPS-4 and GPS-11 beginning about 5 minutes after the shuttle launch and standing well above the noise. These 2 satellites have the closest line-of-sight (LOS) to the shuttle trajectory during its ascent (Fig. 1) and are the only ones we could identify that clearly show such a perturbation.

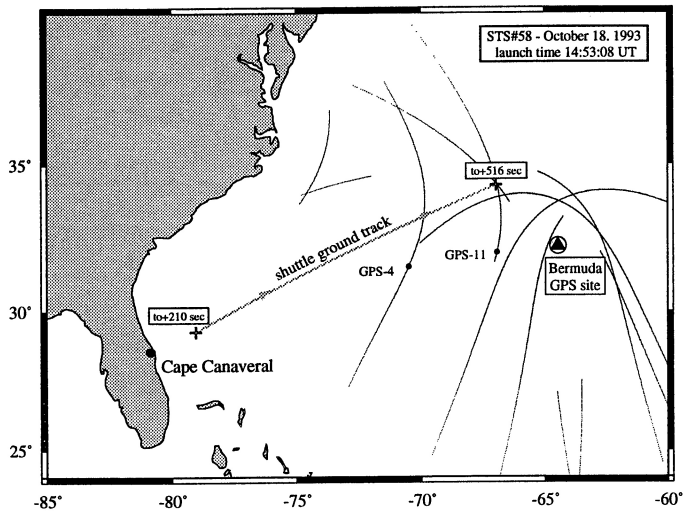


**Figure 1.** STS-58 track over ground during the horizontal part of the Space Shuttle ascent. The Bermuda GPS site and the positions of the GPS satellites during that same time period are indicated. We represent the satellite ground tracks as the projection on the earth's surface of the intersection of the receiver/satellite line-of-sight with the ionosphere at an altitude of 300 km (mean value for the F2 ionospheric region). The black dots labelled GPS-4 and GPS-11 show the location of these two satellites at the time of the shuttle launch.

The perturbation starts at 15:05:01 UT ($t_o + 301$ *sec*) for GPS-4 and 15:07:23 UT ($t_o + 443$ *sec*) for GPS-11 and lasts for about 35 mn. It shows two sub-events separated by 18 mn for GPS-4 and 13 mn for GPS-11. In both cases the first arrival is a small negative pulse, followed by a strong positive pulse that corresponds to the maximum amplitude of the TEC perturbation ($2.5\times10^{15}$ el/m$^2$ for GPS-4 and $3.9\times10^{14}$ el/m$^2$ for GPS-11). It is followed by a first train of oscillatory waves. A second train of oscillatory waves is clearly visible, starting at 15:19:47 UT for GPS-4 and 15:21:36 UT for GPS-11.

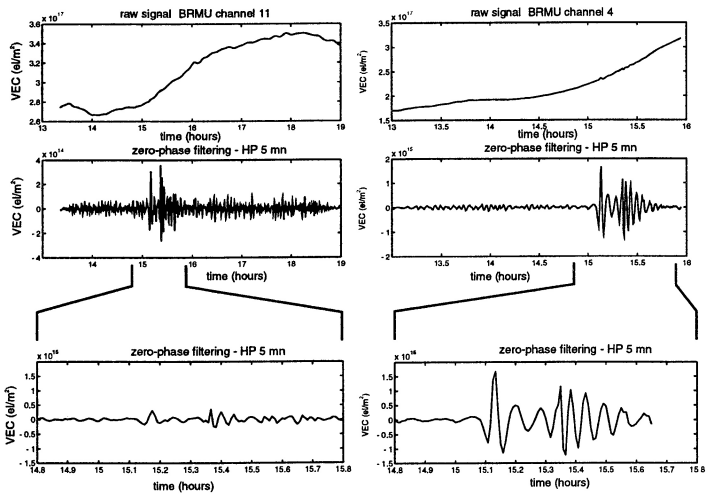


**Figure 2.** Raw and high-pass filtered VEC time series for satellites 4 and 11. The lower boxes show a zoom of the perturbation with the same amplitude scale for both satellites.

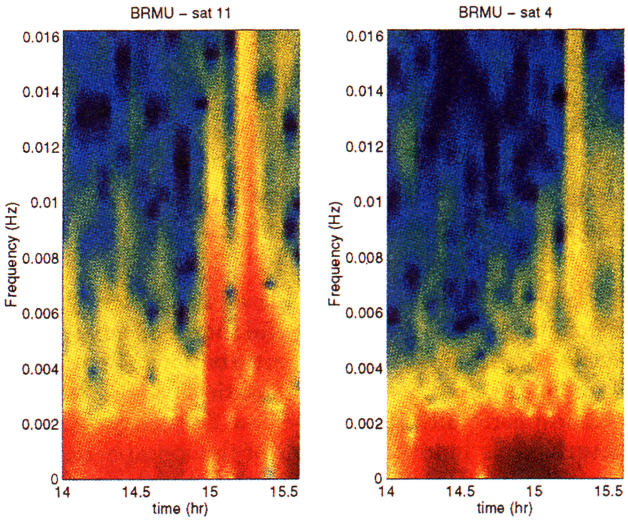


**Figure 3.** Spectrograms of satellite 4 and satellite 11 TEC time series computed using a 15 mn window length and 5 mn steps.

We computed spectrograms for the GPS-4 and GPS-11 time series using a 15 mn window length and 5 mn steps (Fig. 3). The TEC perturbation appears clearly on the spectrograms shortly after 15:00, with two sub-events. Both spectrograms show that the energy of the first sub-event is strongly tapered down for periods lower than 100 sec (frequency >0.01 Hz) whereas the second sub-event has a wider period range including higher frequencies as well.

Several studies have reported atmospheric perturbations caused by rocket ascents, using ground level measurements (Donn *et al.*, 1968; Fehr, 1968; Kashak, 1969; Arendt, 1971), HF ionospheric Doppler sounders (Tolstoy *et al.*, 1970; Zasov *et al.*, 1977; Jacobson and Carlos, 1994), incoherent scatter radar (Noble, 1990), and geosynchronous satellite beacon signals (Li *et al.*, 1994). In a recent publication, Li *et al.* (1994) report ionospheric TEC variations up to $9.6\times10^{13}$ electrons/m$^2$ caused by an acoustic perturbation in the 50 to 150 sec period band after several Space Shuttle ascents, including the STS58 mission. They also identify two arrivals separated by about 15 mn, as Tolstoy *et al.* (1970) had also observed after Apollo launches. Our observations match well these previous reports, which validates our approach based on GPS measurements.

## Interpretation

**The shock front:** Figure 4 shows the distance traveled by the acoustic perturbation between the source (the shuttle) and the LOS as a function of time between $t_1$ and $t_{MECO}$. Since the shuttle velocity is supersonic, we assume the acoustic wave front to propagate perpendicularly to the shuttle trajectory (Li *et al.*, 1994). We therefore calculate the source/LOS distance in a direction orthogonal to the shuttle trajectory. We then assume that the perturbations detected on the LOS have their source at the time of the closest approach between the source and the LOS. The GPS-4 and GPS-11 time series are reported at zero distance on Figure 4 since

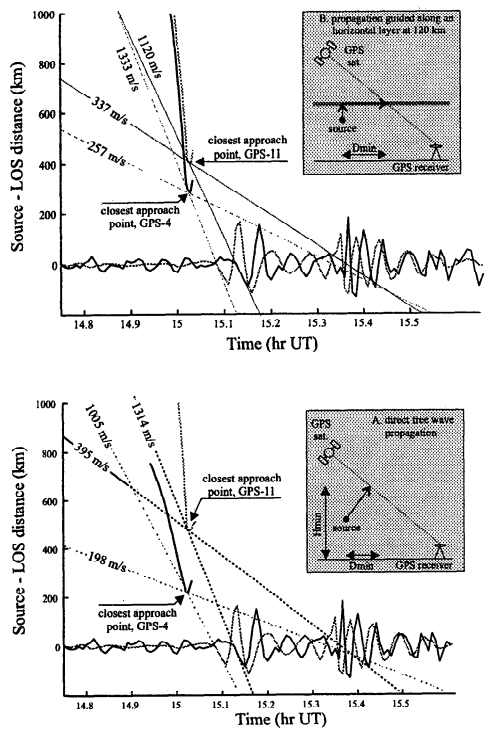


**Figure 4.** Distance travelled by the acoustic perturbation between the source (the shuttle) and the LOS as a function of time between $t_1$ and $t_{MECO}$. Top: case of a free wave propagating from the source up to 100 km followed by a guided wave propagating horizontally at 100 km to the LOS. Bottom: case of the direct propagation of a free wave from the source to the LOS.

they represent the signal recorded along the LOS. A straight line between the arrival time of the perturbations and the closest approach point (dashed lines on Fig. 4) gives the average velocity of the perturbation along its path (Table 1).

For the shock front, we obtain velocities of 1005 m/s for a perturbation travelling below 218 km and 1314 m/s for a perturbation travelling below 477 km. These values correspond to horizontal velocities of 894 m/s and 862 m/s respectively. Greene and Whitaker (1968) have shown that shock fronts are manifested as large non-oscillatory pulse-like disturbances travelling horizontally at about 750 m/s. Although their calculation used the case of a large nuclear explosion and explored the hydrodynamic nonlinearities in a regime which is not necessarily similar to that of the Space Shuttle, these characteristics match the sharp and well-defined first pulse visible on the filtered time series (Fig. 2). Such high-speed shock fronts have also been reported after atmospheric nuclear tests (*e.g.* Broche, 1972). Similarly, Noble (1990) and Li *et al.* (1994) report a direct shock front generated by Space Shuttle launches that propagates with a horizontal phase velocity of 600 to 700 m/s. Tolstoy *et al.* (1970) also report a shock front after Apollo launches and determine a horizontal phase velocity of 700 to 800 m/s. The greater phase velocities that we obtain can be explained by the fact that the GPS measurement integrates the TEC over higher altitudes than other techniques. We propose to interpret this first arrival as the result of the direct propagation of internal acoustic waves excited by the shuttle blast.

**The oscillatory perturbation:** Waveform simulations of ionospheric perturbations generated by shuttle launches have so far been unable to explain the oscillatory regime that follows the shock front (*e.g.* Li *et al.*, 1994). A common theoretical explanation, however, is to invoke the effect of guided waves, excited by the shock front when it reaches an atmospheric interface that supports guided modes such as the mesopause (around 100 km altitude) or the thermocline (around 120 km altitude) (*e.g.* Harkrider, 1964; Greene and Whitaker, 1968; Tolstoy *et al.*, 1970; Francis (1975); Broche (1977); Richmond, 1978; Nalesso and Jacobson, 1993). We examine hereafter how these mechanisms can be applied to our observations.

*First wave train ($W_1$):* In the hypothesis of a perturbation propagating up to 120 km followed by a guided wave propagating along an horizontal atmospheric guide at 120 km (Fig 4 bottom), we obtain average phase velocities between 300 m/s and 500 m/s for $W_1$, close to the sound velocity at 120-150 km altitude. Such a wave will reach the LOS earlier than a wave guided at about 100 km (mesopause level, explanation proposed for the second wave train $W_2$, *cf. infra*) because the sound velocity is lower at these altitudes. This explanation would also account for the differences in frequency content between $W_1$ and $W_2$ (Fig. 3). Indeed, acoustic waves are attenuated with altitude as a function of their frequency (*e.g.* Blanc, 1985). In particular, frequencies in the 0.1-0.01 Hz range are totally attenuated at 130-160 km. A large part of the frequency content of $W_1$ corresponds to the acoustic domain ($> 0.0035$ Hz, Fig. 3). In addition, our observations show a lower frequency content for $W_1$ than $W_2$ with a cut-off frequency of about 0.01 Hz for $W_1$ (Fig. 3). This suggests a propagation of $W_1$ at higher altitudes than $W_2$.

*Second wave train ($W_2$):* Li *et al.* (1994) interpreted the second wave train as the reflection of the acoustic perturbation from the ground. However, Calais and Minster (1995) identified ionospheric electron content variations caused by an earthquake that also show two wave trains separated by about 15 mn. The second arrival, in this latter case, cannot be explained by a ground reflection. In the hypothesis that both phenom-

**Table 1.** Closest approaches between the shuttle trajectory and GPS-4 and GPS-11 LOS. $D_{min}$ (km) is the shuttle/LOS distance, $T_{min}$ (hours UT) is the time of the closest approach, and is $H_{min}$ (km) the altitude of the closest approach point on the LOS at $T_{min}$. The first two rows correspond to the case of a direct free wave propagation (Fig. 4A), rows 3 and 4 correspond to the case of a propagation guided horizontally at 100 km (Fig. 4B).

| sat | $D_{min}$ | $T_{min}$ | $H_{min}$ | $V_1$ | $V_2$ |
|---|---|---|---|---|---|
| GPS-4 | 208 | 15.0172 | 218 | 1005 | 198 |
| GPS-11 | 467 | 15.0247 | 477 | 1314 | 395 |
| GPS-4 | 270 | 15.0247 | 100 | 1273 | 246 |
| GPS-11 | 354 | 15.0247 | 100 | 973 | 293 |

ena are the result of the same physical process, this would rule out Li *et al.*'s interpretation. An alternate hypothesis is to consider this perturbation as the result of a wave propagating from the source up to 100 km (mesopause level) as a direct free wave, followed by a guided wave propagating along an horizontal atmospheric guide at 100 km (Fig. 4 top). In this hypothesis, we obtain a phase velocity of 246 m/s and 293 m/s for GPS-4 and GPS-11 respectively, consistent with the sound velocity around 100 km.

## Conclusion

Using GPS data collected on Bermuda island, we detected a perturbation of the ionospheric electron content caused by the ascent of the Space Shuttle during the STS-58 mission. The good signal-to-noise ratio allowed us to clearly image the waveform characteristics of this perturbation and to compare it with previous observations and theoretical models. We show that this complex perturbation can be explained by an impulsive high-velocity shock front that propagates as a direct internal wave, followed by oscillatory guided waves probably excited by the primary shock wave and propagating along horizontal atmospheric interfaces at 120 km altitude (thermocline) and 100 km altitude (mesopause).

Our observation of the STS-58 perturbation was limited by the 30 sec sampling rate of the GPS receiver and by the poor GPS coverage of the region overflown by the Space Shuttle. However, the detection level achieved by the GPS technique leads us to believe that it has the potential for investigating other sources of ionospheric perturbations as well as for studying acoustic-gravity waves and coupling processes in the upper atmosphere.

**Acknowledgments.** We thank Yehuda Bock and Jeff Behr from the Scripps Orbit and Permanent Array Center for making the Bermuda GPS data available to us; Stella Luna from the NASA Lyndon B. Johnson Space Center, Office of Public Affairs, for providing us with the ascent data of the STS-58 mission; Charles Archambeau and John Davies for interesting discussions and for providing us with a manuscript of their theoretical work in advance of publication; Stephen Warshaw and Jennifer Haase for useful advices and discussions. The careful reviews by three anonymous reviewers are much appreciated. This work was supported by the National Aeronautics Administration Grant No. NAG 5-1910.

## References

Arendt, P.R., Ionospheric undulations following Apollo 14 launching, *Nature, 231*, 438-439, 1971.

Blanc, E., Observations in the upper atmosphere of infrasonic waves from natural or artificial sources: a summary, *Annales Geophysicae*, 3, 6, 673-688, 1985.

Broche, P., Propagation non linéaire et couplage ionosphérique des ondes atmosphériques engendrées par une explosion nucléaire, *AGARD Conf. Proc., 115*, 1972.

Broche, P., Propagation des ondes acoustico-gravitationnelles excités par des explosions, *Ann. Geophys., 33*, 281-288, 1977.

Calais, E., and J.B. Minster, GPS detection of ionospheric perturbations following the January 17, 1994, Northridge earthquake, *Geophys. Res. Lett., 22*, 1045-1048, 1995.

Donn, W.L., E. Posmentier, U. Fehr, and N.K. Balachandran, Infrasound at long range from Saturn V, *Science, 162*, 1116, 1968.

Fehr, U., Propagating energy in the upper atmosphere including lower ionosphere generated by artificial sources, in *Acoustic-Gravity Waves in the Atmosphere: Symposium Proceedings*, edited by T.M. Georges, U.S. Government Printing Office, Washington D.C., 1968.

Francis, S.H., Acoustic-gravity modes and large-scale traveling ionospheric disturbances of a realistic, dissipative, atmosphere, *J. Geophys. Res., 78*, 2278-2301, 1973.

Francis, S.H., Global propagation of atmospheric gravity waves: a review, *J. Atmos. Terr. Phys.*, 37, 1001-1054, 1975.

Greene, J.S., and W.A. Whitaker, Theoretical calculations of traveling ionospheric disturbances generated by low-altitude nuclear explosions, in *Acoustic-Gravity waves in the Atmosphere: Symposium Proceedings*, edited by T.M. Georges, U.S. Government printing Office, Washington D.C., 1968.

Harkrider, D.G., Theoretical and observed acoustic-gravity waves from explosive sources in the atmosphere, *J. Geophys. Res., 69*, 5295, 1964.

Jacobson, A.R., and R.C. Carlos, Observations of acoustic-gravity waves in the thermosphere following Space Shuttle ascents, *J. Atmos. Terr. Phys.*, 56, 4, 525-528, 1994

Kaschak, G.R., Long-range supersonic propagation of infrasonic noise generated by missiles, *J. Geophys. Res., 72*, 4559, 1967.

Klobuchar, J.A., Ionospheric time delay effects on earth-space propagation, *Handbook of Geophysics and The Space Environment*, edited by A.S. Jursa, chap. 10.8, 1084-1088, U.S. Air Force, Washington D.C., 1985.

Li, Y.Q., A.R. Jacobson, R.C. Carlos, R.S. Massey, Y.N. Taranenko, and G. Wu, The blast wave of the Shuttle plume at ionospheric heights, *Geophys. Res. Lett., 21*, 2723-2740, 1994.

McLeod, M.A., Sporadic E theory, 1. Collision-geomagnetic equilibrium, *J. Atmos. Sci., 23*, 96-109, 1966.

Nalesso, G.F., and A.R. Jacobson, On a mechanism for ducting of acoustic and short-period acoustic-gravity waves by the upper atmospheric thermocline, *Annales Geophysicae, 11*, 372-376, 1993.

Noble, S.T., A large-amplitude traveling ionospheric disturbance excited by the Space Shuttle during launch, *J. Geophys. Res., 95*, 19,037-19,044, 1990.

Richmond, A.D., The nature of gravity wave ducting in the thermosphere, *J. Geophys. Res., 83*, 1385, 1978.

Tolstoy, I., H. Montes, G. Rao, and E. Willis, Long-period sound waves in the thermosphere from Apollo launches, *J. Geophys. Res., 75*, 5621-5625, 1970.

Zasov, G.F., V.D. Karlov, T.Y. Romanchuk, G.K. Solodovnikov, G.N. Tkachev, and M.G. Trukhan, Observations of disturbances in the lower ionosphere during Soyuz-Apollo experiments, *Geomagn. Aeron.*, Engl. Transl., 17, 234, 1977.

E. Calais, CNRS-Sophia Antipolis, UMR Géosciences, 250 Rue A. Einstein, 06560 Valbonne, France, calais@faille.unice.fr

J.B. Minster, Scripps Institution of Oceanography, IGPP 0225, University of California, San Diego, 9500 Gilman Drive, La Jolla, CA 92093-0225, USA, jbminster@ucsd.edu

(received 02/12/95; revised 11/04/96; accepted 12/04/96.)